Mechanical behaviour and physical ageing of semi-crystalline polymers: 4

L. C. E. Struik*
Plastics and Rubber Research Institute TNO, PO Box 71, 2600 AB Delft, The Netherlands
(Received 29 March 1988; revised 18 October 1988; accepted 1 November 1988)

It is shown that for some semi-crystalline polymers (PP, HDPE at 20°C and higher) the effect of previous physical ageing on creep decreases with increasing level of stress, as found previously for amorphous polymers. This finding suggests that for semi-crystalline materials, high stresses can erase previous ageing and can rejuvenate the material. As a consequence, the methods developed for the prediction of long term creep could be generalized to the high stress regime. It is further shown that for compression moulded, annealed, PP, the upper T_g, T_g^U, lies around +100°C. Moreover the effect of stress level on ageing disappears for temperatures above 100°C. Finally, it is shown that a change from compression to injection moulding strongly influences the creep properties. The material becomes softer (factor of 2–3) and T_g^U drops by at least 25°C. This overall effect on T_g^U seems more important (for the creep properties) than the frozen-in stresses and orientations.

(Keywords: semi-crystalline polymers; mechanical behaviour; ageing)

INTRODUCTION

This is the last of a sequence of four papers[1–3]. Some additional data will be presented on two commercial PPs and one HDPE which were investigated after completion of the study reported in references 1–3. The work deals with the effect of ageing on the non-linear creep at high stress levels and with the effect of injection *versus* compression moulding on the creep properties. The paper concludes with a general discussion of the results obtained in the four papers of the sequence.

EXPERIMENTAL

Materials

The materials studied were received through DSM. Two types of PP were investigated: P83M10 (DSM) and Carlona GMT 67 (Shell). The HDPE sample was a Stamylan 9309 from DSM.

For PP, we investigated compression moulded as well as injection moulded samples. For HDPE only injection moulded samples were tested. Compression moulding was performed by DSM, injection moulding by TNO. The moulding conditions were as follows.

Compression moulding. (PP, sheets of 200 × 50 × 4 mm) press temperature 210°C; conditions: 7 min without pressure, 5 min under 10 bar, 5 min under 50 bar followed by cooling under 800 bar at 40°C/min. The sheets showed some marbly texture which intensified during creep at high strains (few percent). After moulding, the sheets were annealed between 6 mm thick glass plates for 1 night at 140°C and subsequently cooled to room temperature in 6 h.

Injection moulding. (PP and HDPE). The sheets (90 × 90 × 2 mm) were produced with a Maurer M100 machine, provided with a 50 mm screw and valve operated injection nozzle. The processing conditions are summarized in *Table 1*. Two series of sheets were made, the first with a mould temperature, T_m of 20°C, the second with a T_m of 60°C.

Creep samples

All samples were milled to rectangular strips of 200 × 7 × 1 mm (compression mouldings) or 85 × 10 × 2 mm (injection mouldings). With the compression moulded samples, the ageing was studied after requenching from 130°C to the measuring temperature in the oven of the creep tester. Therefore the storage time of the samples in the laboratory was irrelevant. For the injection moulded samples, no additional requenching was made. Consequently, the storage period at room temperature adds to the ageing period.

To prevent problems, all injection moulded sheets were cooled to and stored at −196°C immediately after moulding. The sheets were only brought to room temperature for the milling of the strips. The milling time was minimized and noted for each sample. For the tests at 23°C, the milling time (about 15 min) was added to the ageing time. For the tests at 40 and 70°C this was not done, because the 15 min ageing at 23°C will hardly influence the behaviour at 40 and 70°C[2,4].

Creep testing

All tests were done with the automatic tensile creep tester described in Appendix A.5 of reference 4 and with the long term tensile creep testers described in Appendix A.6 of reference 4. Particularly for the injection moulded samples, the creep strains should be corrected for spontaneous shrinkage. This shrinkage (0.1–0.3% between

* Now at: DSM Research, PO Box 18, 6160 MD Geleen, The Netherlands

0032-3861/89/050815-16$03.00

Table 1 Injection moulding conditions. For the two mould temperatures (20 and 60°C), all conditions were the same, except when numbers in parentheses are given; these refer to $T_m = 60°C$

	P83M10	Carlona GMT 67	Stamylan 9309
Cylinder temperature, °C			
zone 1	195	195	195
zone 2	205	205	205
zone 3	210	210	210
zone 4	230	230	230
zone 5	240	240	240
zone 6	240	240	240
Nozzle temperature, °C	245/250	245/250	245/250
Injection time, s	0.5	0.5	0.6
After pressure time, s	5	7	10
Cooling time, s	12	12	10.9 (12.0)
Waiting time, s	2	2	2
Cycle time, s	24	25	27 (28)
Injection pressure, bar	55 (45)	55	50
After pressure, bar	35	35	30
Closing force, kN	1000	1000	1000

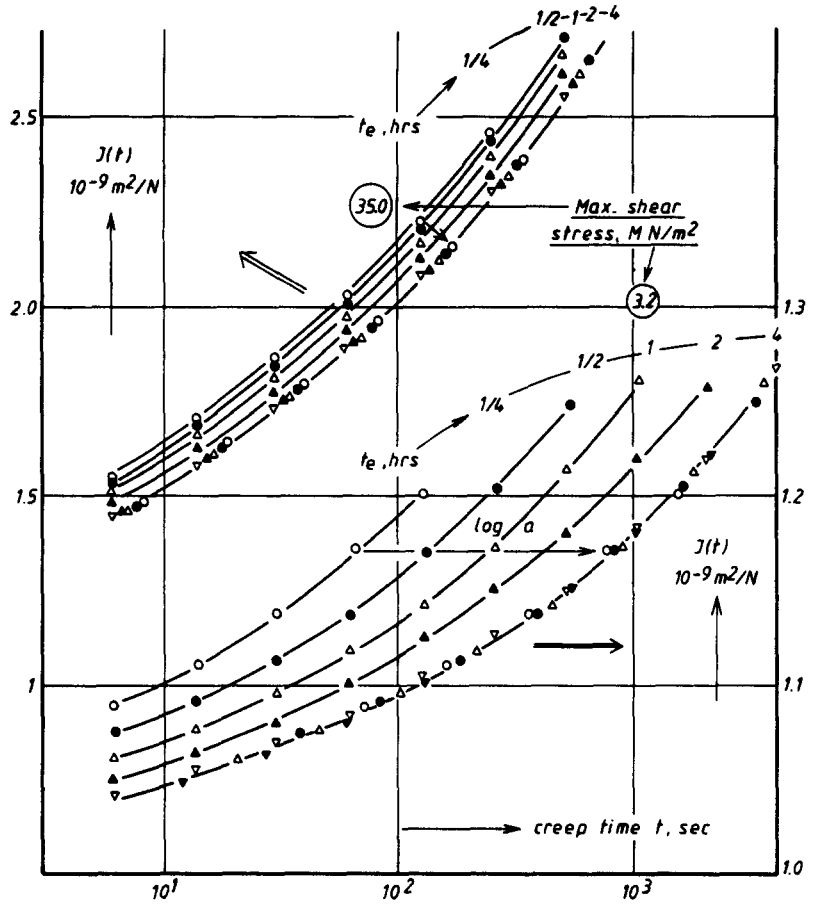

Figure 1 Shear creep compliance $J(t)$ of rigid PVC at various times t_e elapsed after quenches from 90 to 20°C. For the lowest stress, the tests were done sequentially after a single quench, for the higher stress level, the sample was reheated to above T_g between each two tests. This procedure yields the same results as when a new sample was used for each creep test[4,6]. The master curves were obtained by shifting. The arrows give the shifting direction. The stress level indicated is the maximum shear stress in the surface of the sample (rectangular bar). Note that the compliance scales are different for the two stress levels

0.5 and 1000 h after moulding) was determined by separate experiments under zero stress. The relative importance of the shrinkage correction decreases with increasing stress level (creep strain). So, if the corrections were omitted, one would erroneously conclude that the creep behaviour is non-linear, particularly at very low strains.

CREEP AT HIGH STRESS LEVELS

Effect of stress level on ageing

In Chapter 8 of reference 4 we reported that, for amorphous polymers, high stresses can erase previous ageing. Some experimental results are summarized in *Figures 1* and *2*. *Figure 1* shows creep data for rigid PVC

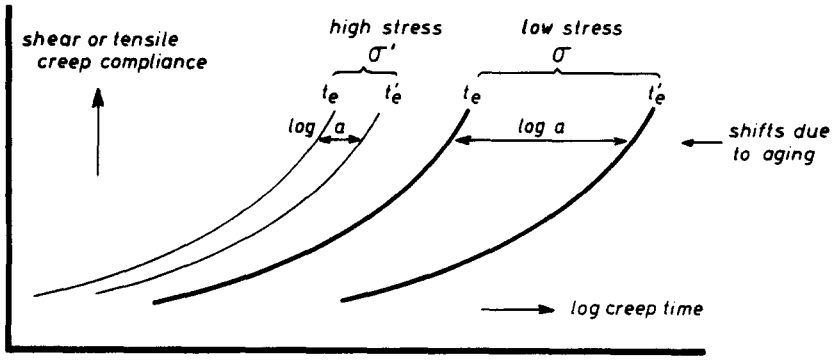

Figure 2 Schematic illustration of the effects of ageing and high stresses on creep. t_e and t'_e are two different ageing times, $t'_e > t_e$. The figure only shows the horizontal shifting of the creep curves; the vertical shifts (cf. *Figure 1*) are omitted. Reproduced from ref. 4 with permission

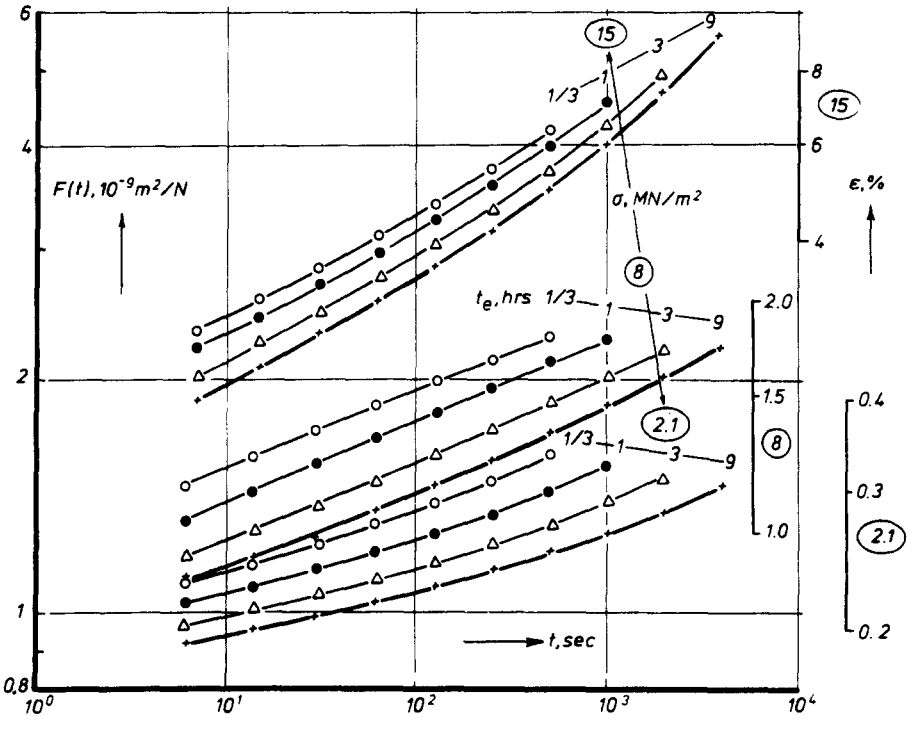

Figure 3 Tensile creep of compression moulded PP, P83M10, quenched from 130 to 23°C and (creep) tested after times t_e (elapsed at 23°C) of 1/3, 1, 3 and 9 h. For the lowest stress, the tests were done in succession on one sample after a single quench. This is allowed because effects of repeated testing are absent at low stress levels[6]. For the higher stress levels, a new sample was used for each creep test. The tests were done at 2.1, 5, 8, 11 and 15 MN/m² but the data at $\sigma = 5$ and 11 MN/m² have been omitted from this figure. ○, ●, △, and + denote the t_e of 1/3, 1, 3 and 9 h, respectively. The right-hand scale gives the strains; the corresponding stress levels are circled. The tests were done at 23, 40, 60, 80, 100 and 120°C; only the results at 23, 60 and 120°C are given in *Figures 3–5* respectively

at various times t_e, elapsed after a quench from 90 to 20°C. It is quite clear that at high stress levels the shifts due to changes in t_e are less than at low stress levels. However, the superposability of the creep curves measured at various t_e values remains (see the master curves). Throughout this paper, the effect of ageing on creep is discussed in terms of simple horizontal shifts or combinations of horizontal and vertical shifts. The background is given in the earlier papers of this series (ref. 1–3).

Results as shown in *Figure 1* were obtained in torsion as well as in tension for rigid PVC, PS and PC at a number of temperatures below T_g. A summary of the results is given in *Figure 2*. Full details can be found in section 8.1 of reference 4. *Figure 2* shows that the horizontal shift $\log a$ due to a change in t_e decreases with increasing stress. Consequently, shift rate $\mu = \mathrm{d}\log a/\mathrm{d}\log t_e$ decreases with increasing σ. The explanation proposed in ref. 4 was that the large deformation processes, caused by the high stress, generate free volume and so rejuvenate the sample and partially erase the previous ageing. For a comprehensive discussion, see reference 5.

It is an interesting question whether similar effects can be found in semi-crystalline polymers. In the model of reference 1, we try to explain the behaviour of these materials from phenomena in the amorphous phase. So, according to this model a behaviour as shown in *Figures 1* and *2* should also be found in materials such as HDPE and PP, at least in regions 1–3.

The experimental results are given in *Figures 3–11*.

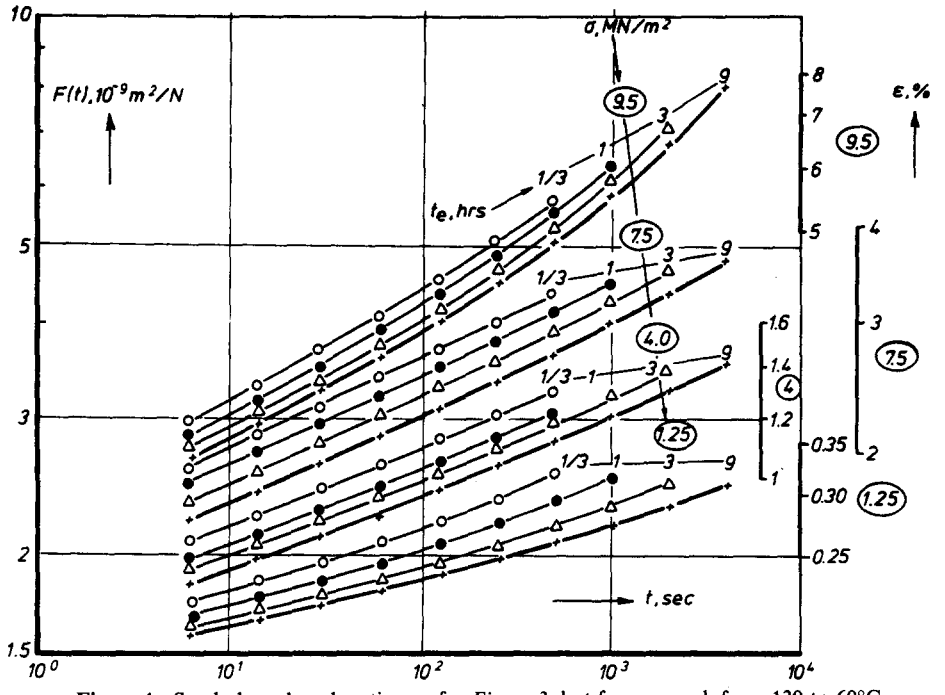

Figure 4 Symbols and explanation as for *Figure 3*, but for a quench from 130 to 60°C

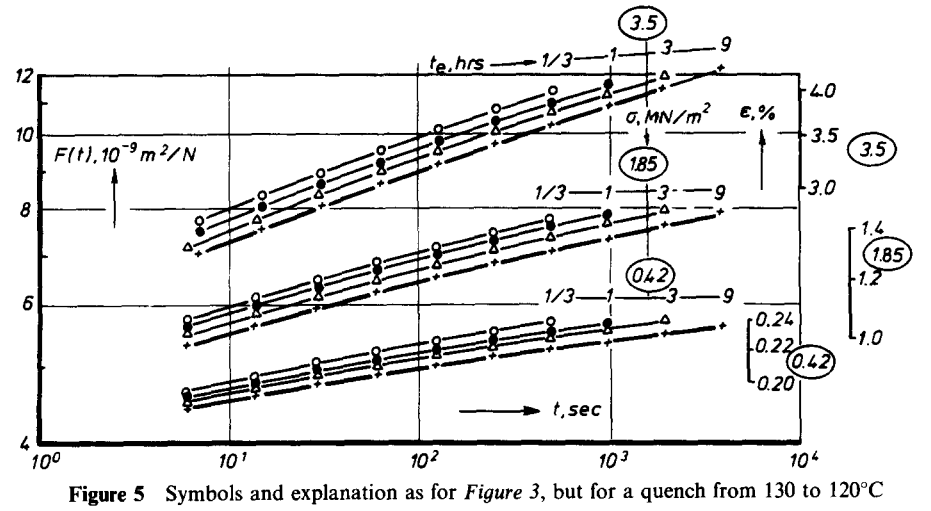

Figure 5 Symbols and explanation as for *Figure 3*, but for a quench from 130 to 120°C

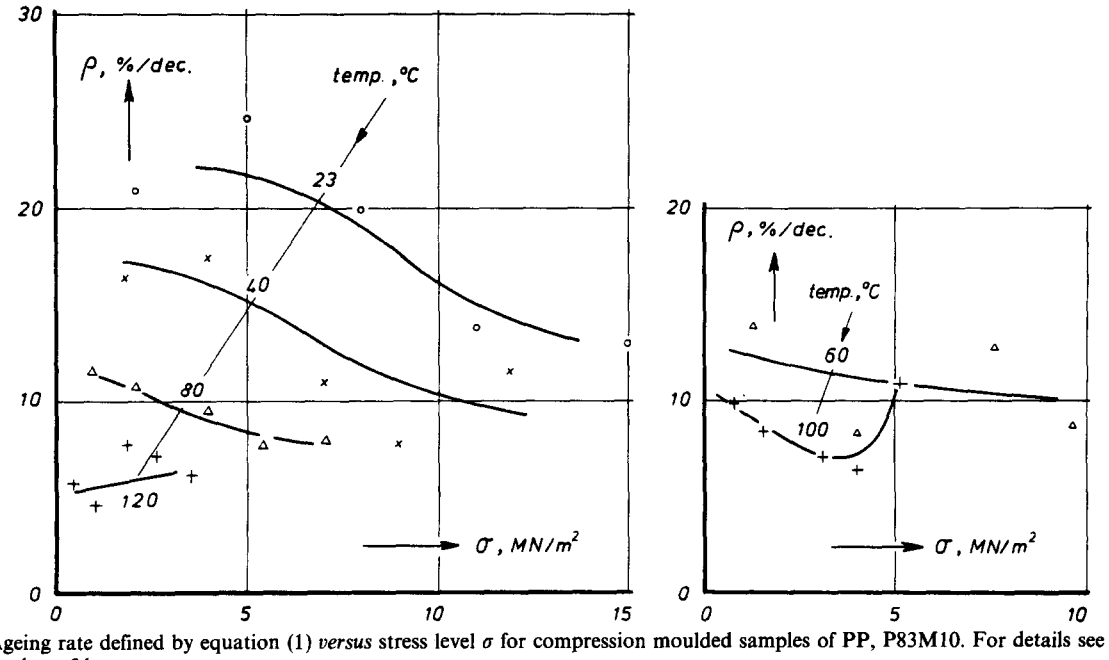

Figure 6 Ageing rate defined by equation (1) *versus* stress level σ for compression moulded samples of PP, P83M10. For details see text; ρ refers to $t = 10^3$ s and $t_e = 3$ h

Figures 3–5 show data, similar to those of *Figure 1*, but for the compression moulded sample of PP, tested at 20–120°C. For the lower temperatures we observe the same effect as for PVC (*Figure 1*). The ageing effects diminish with increasing stress. At 100–120°C, this effect disappears, however (we will return to this point later).

The effect of ageing can be characterized by parameter ρ defined as:

$$\rho = -\frac{100}{F(t)}\frac{\mathrm{d}F(t)}{\mathrm{d}\log t_e} \qquad (1)$$

for some constant value of creep time t. In fact, ρ gives the percentage change in F per tenfold increase in t_e.

Figures 6 and *7* give ρ for a creep time t of 1000 s and at a t_e of 3 h. *Figure 6* shows ρ *versus* stress level σ, *Figure 7* gives ρ *versus* the strain ε reached at $t = 10^3$ s and $t_e = 3$ h. For temperatures up to 80°C, ρ clearly decreases with increasing σ or ε.

Another way to characterize the magnitude of the ageing effects is to determine the double-logarithmic shift rate $\mu = \mathrm{d}\log a/\mathrm{d}\log t_e$. It specifies the horizontal component of the rate at which the creep curves shift along the logarithmic time scale with increasing value of t_e (cf. *Figure 2*). For amorphous polymers, μ sharply decreases with the stress level (Figures 59–62 of ref. 4); the same is observed for PP in *Figure 8*. Similar results were obtained on injection moulded samples of PP and HDPE. A typical ageing test on an injection moulding is presented in *Figure 9*. Plots of μ *versus* ε or σ are given in *Figure 10* for PP, and in *Figure 11* for HDPE.

The data in *Figures 3–11* convincingly show that, for semi-crystalline polymers, the ageing effects also become less pronounced with increasing stress. Moreover the data show that the μ *versus* ε relationship appears less sensitive to changes in temperature than the μ *versus* σ relationship. In addition, although ρ and μ strongly decrease with increasing stress (or strain), these quantities do not reach zero. So, for the stress levels used in *Figures 3–11*, the ageing effects do not completely disappear. The same was observed for amorphous polymers[4]. For these

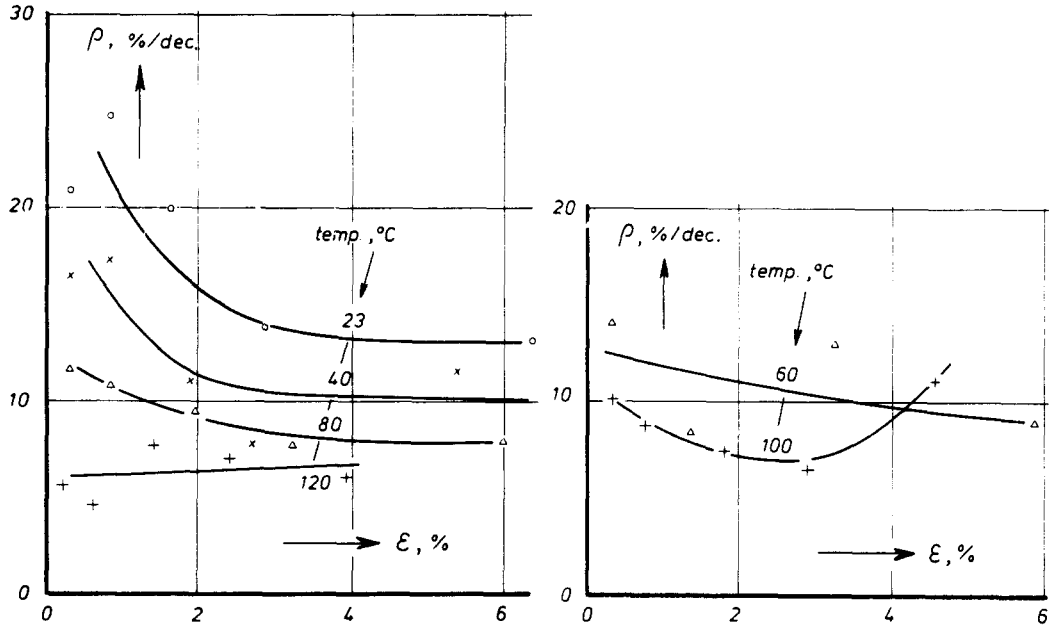

Figure 7 As *Figure 6*, but ρ is plotted *versus* the strain ε reached at $t = 10^3$ s and $t_e = 3$ h

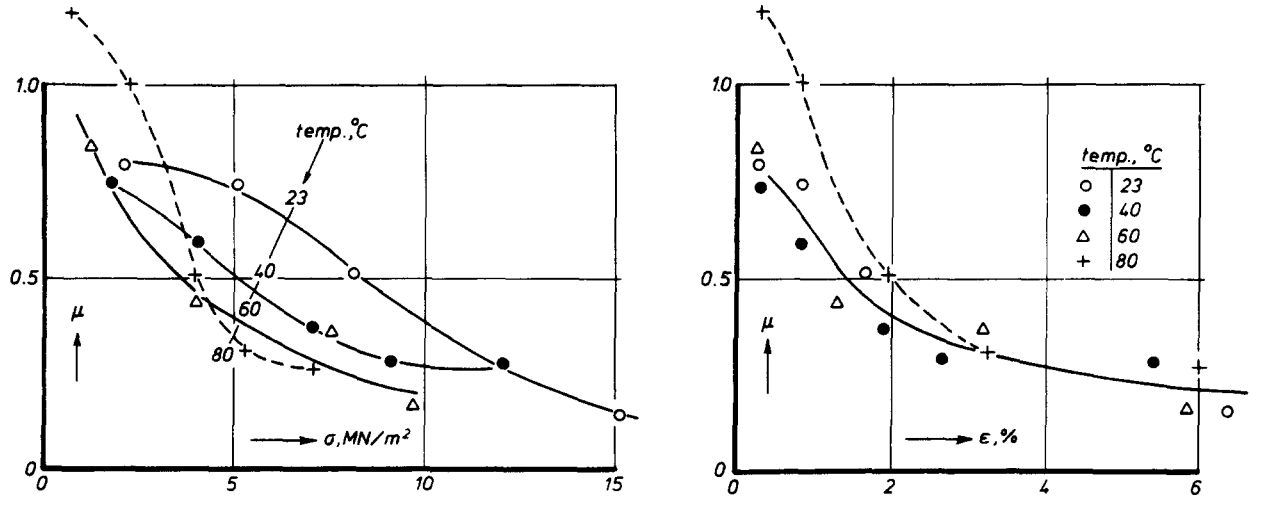

Figure 8 Shift rate μ *versus* stress (left) or strain (right). The t and t_e values are as in *Figures 6* and *7*

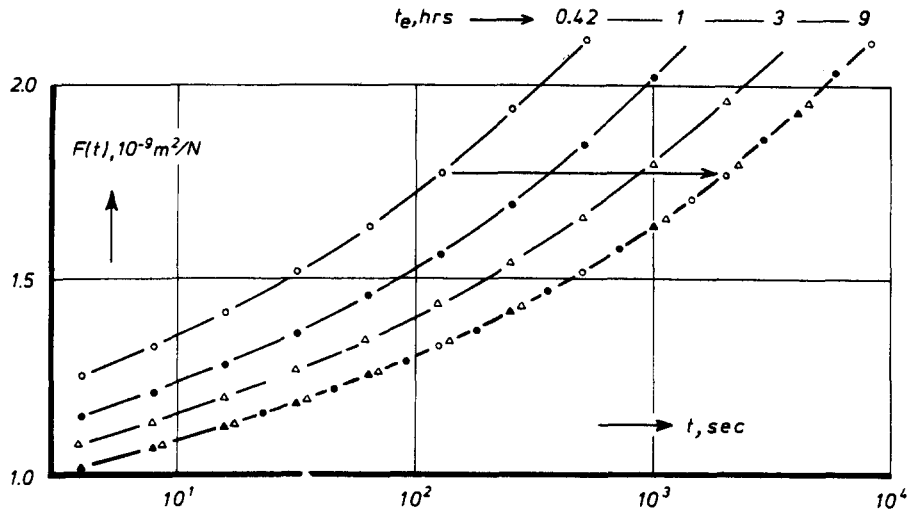

Figure 9 Small-strain tensile creep ($\sigma = 1.33\,MN/m^2$) for injection moulded PP, P83M10 (mould temperature $T_m = 60°C$, sample taken parallel to flow direction). After moulding, the sample was stored at $-196°C$, except for the milling period of 0.25 h at 23°C. Next, four successive small strain creep tests were done at 23°C using the same sample. The t_e values denote the total time at 23°C, and include the milling period. The master curve was obtained by horizontal and vertical shifts. The arrow denotes the shifting direction (the vertical shifts were zero in this case). Similar tests were done for other stress levels and for measuring temperatures of 40 and 70°C. For the higher stress levels, a new sample was taken for each test. For 40 and 70°C, the milling period at 23°C was ignored in the t_e value (see text)

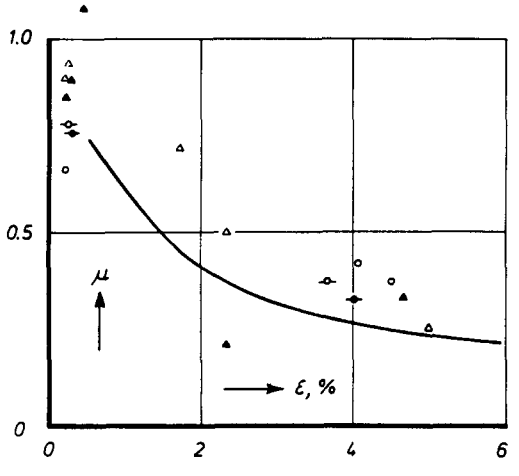

Figure 10 Shift rate μ *versus* strain level ε at $t = 10^3$ s and $t_e = 3$ h for injection moulded samples taken parallel (‖) or perpendicular (⊥) to the flow direction in the mould. T_m denotes the mould temperature (during injection moulding), T is the test temperature. The symbols are defined below. The curve shown is the (lower) curve in *Figure 8*, and refers to compression moulded PP

Symbol	Material	T_m (°C)	T (°C)	Orientation
○	P83M10	20	23	‖
△	P83M10	60	40	‖
▲	P83M10	60	40	⊥
—○—	Carlona GMT 67	20	23	‖
—●—	Carlona GMT 67	20	23	⊥

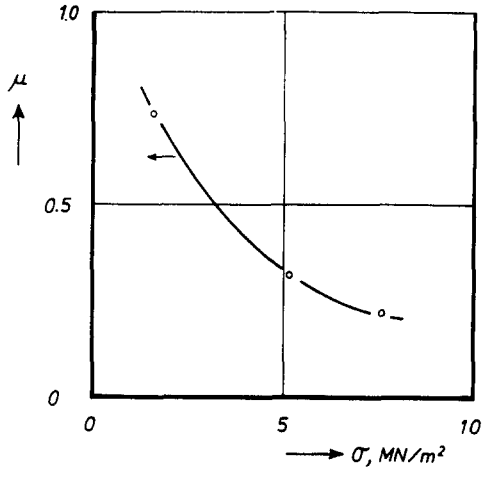

Figure 11 As *Figure 10*, but for HDPE, Stamylan 9309. $T_m = 20°C$; ‖; $T = 23°C$; μ is plotted *versus* the stress level σ

materials the effect of previous ageing seems to disappear only when the yield stress is reached.

Long term creep

The methods for predicting the small-strain long term creep of amorphous and semi-crystalline polymers[3,4] were based on the kinetics of ageing. After a quench, the mobility M (proportional to the creep rate) decreases with age t_e. If $\mu = 1$, M decreases inverse proportionally with t_e. If the creep test is started at t_e, the age after some creep time t will be $t_e + t$, and M will have decreased ($\mu = 1$) from M_{t_e} at $t = 0$ to $M_{t_e}/(1 + t/t_e)$ at t. For $t \gg t_e$, the changes in M are insignificant and we find the momentary creep curve[4]. If $t > t_e$, M begins to decrease rapidly, the creep is decelerated and the creep curves become almost straight on $\log t$ scale. This linearity on $\log t$ scale is a direct consequence of the ageing[4,5]; it sets in for $t \sim t_e$.

For amorphous polymers, the results discussed earlier led to the following picture (see Chapter 8 and section 11.5 of reference 4). Application of a high stress is to some extent comparable to a brief heating to above T_g, followed by a quench. The large deformation processes generate free volume. The sample is rejuvenated and the previous ageing is (partially) erased. The production of free volume, however, is coupled to the deformation rate and in creep this rate decreases with time. So, after some creep time t_1, the free volume production can no longer

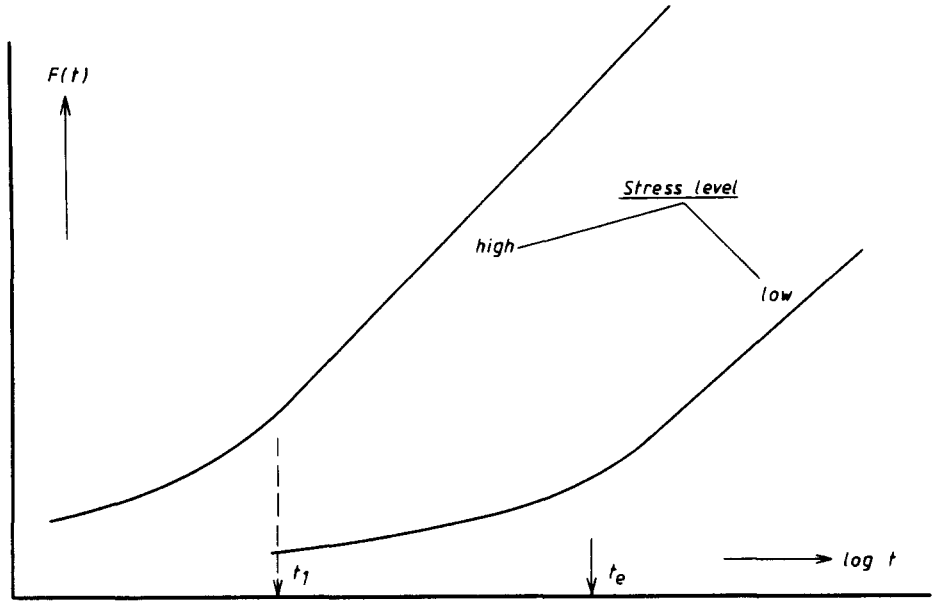

Figure 12 Effect of the stress level on creep compliance $F(t)=\varepsilon(t)/\sigma_0$; ε is the strain, σ_0 the constant stress. For very low stresses (spontaneous ageing), the $F(t)$ *versus* $\log t$ curve becomes straight for $t>t_e$. For high stresses, the straight line region sets in at $t_1<t_e$ because of stress activated ageing. For details see text

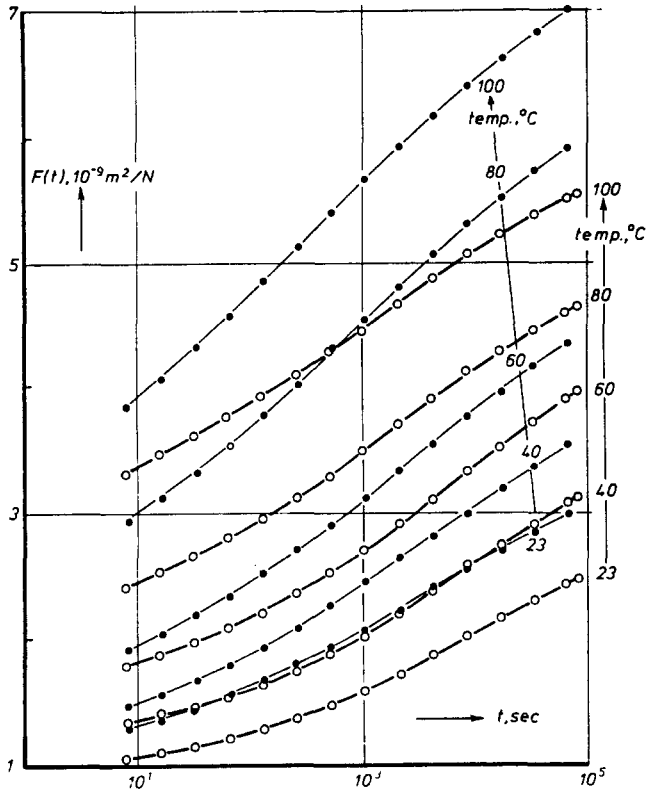

Figure 13 Long term tensile creep of compression moulded PP, P83M10. The tests were started 1 h after a quench from 130°C to the measuring temperature. ○, low stress; final strain ~0.5%; ●, high stress; final strain 2–2.5%

compete with the normal volume-relaxation (free volume annihilation) process. Consequently, a reactivated ageing sets in for $t>t_1$ and mobility M will vary (if $\mu=1$) according to $M=M(t_1)/(1+t/t_1)$.

As a result, the high stress creep curve will have the same appearance as a long term creep curve at small strains. It will be more or less straight and it can be extrapolated linearly. The onset of the straight line region is at t_1, and t_1 is shorter than t_e, the higher the stress (see *Figure 12*). The theory for this effect is given in section 11.5 of reference 4 together with experimental data on rigid PVC.

The results presented previously suggest that rejuvenation and reactivation of ageing will also occur in semi-crystalline polymers. So, for such materials we also expect the behaviour depicted in *Figure 12*. Some experimental data are shown in *Figures 13–15*. The first figure shows creep curves for PP at 23–100°C and a t_e of 1 h; the maximum t/t_e ratio is 22. Inspection shows a satisfactory similarity with *Figure 12*. All creep curves are only slightly curved at long times, and the 'straight' line region sets in earlier for the high than for the low stress. Similar conclusions can be drawn from *Figures 14* and *15*, which contain data which are really long term (t/t_e becomes 3000). Other long term data are given in *Figures 20, 21* and *24*.

The present results show that, for semi-crystalline polymers, the methods developed for predicting the long term creep[3,4] can also be generalized to the non-linear high stress regime. It should, however, be realized that, as for amorphous polymers, these methods only refer to the gross overall deformation of the sample. When localized deformations occur (crazes, shear bands and cracks) the methods lose their applicability.

REGION 4 BEHAVIOUR OF PP (COMPRESSION MOULDED SAMPLES)

In reference 1, we introduced the four regions of characteristic behaviour. Because of the interaction between the amorphous and crystalline phases, there will be a distribution of T_g values, between a lowest value T_g^L and a highest value T_g^U. In view of this, we defined four regions: region 1: $T<T_g^L$; region 2: $T\sim T_g^L$; region 3: $T_g^L<T<T_g^U$ and region 4: $T\geqq T_g^U$. In region 4, the amorphous phase is completely rubbery.

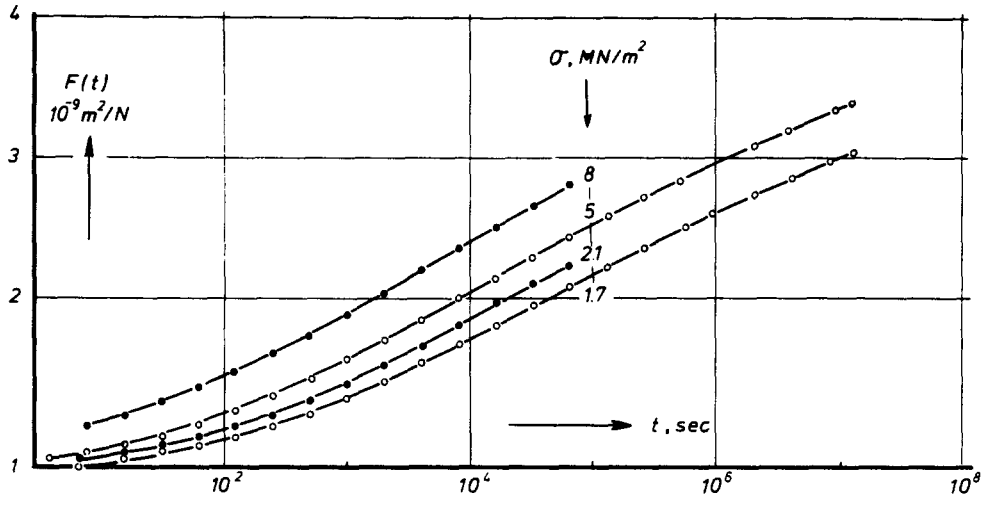

Figure 14 Explanation for *Figure 12*, but in this case some tests were continued to 3000 h; measuring temperature $T=23°C$

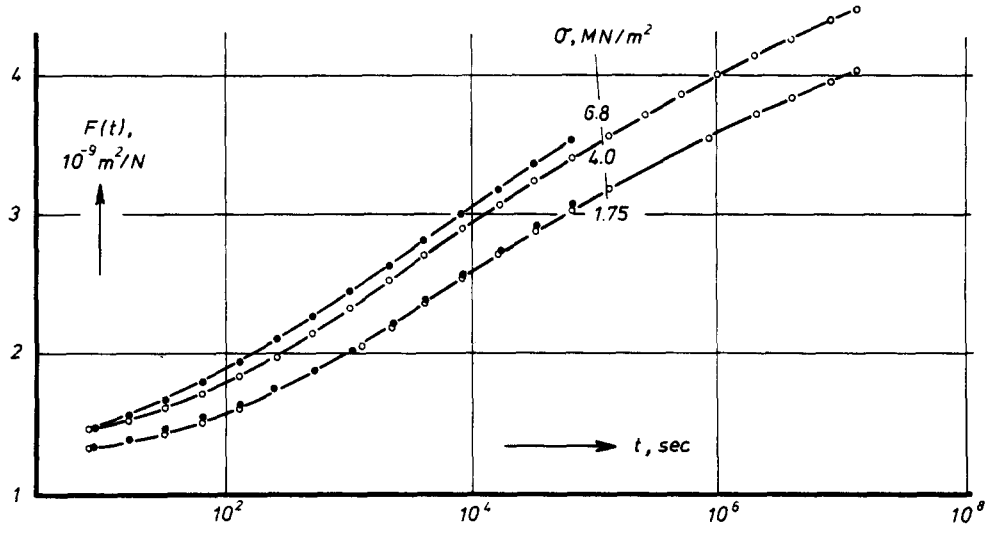

Figure 15 Explanation as for *Figure 14*, but in this case $T=40°C$

Until now, we found a region 4 behaviour for LDPE only (Figure 20 of ref. 2). For the other materials, the measuring temperatures were too low. In the present work, we have observed a region 4 behaviour in compression and injection moulded samples of PP and in the injection moulded HDPE. The results on the compression moulded PP will be discussed first.

The creep data are shown in *Figures 16A–F*. These diagrams should be compared with Figures 8 and 11–13 of reference 1. At lower temperatures, we observe the usual picture: a region 2 behaviour (downward shifts) at 23°C, region 3 behaviour (upward shifts) at 60 and 80°C, and a transition from region 2 to 3 at 40°C. Exactly the same was found in reference 1. However, at 100°C the curves are no longer superimposable (*Figure 16E*) and at 120°C a superposition is only possible in a double-logarithmic diagram (*Figure 16F*). The last figure should be compared with *Figure 13* for LDPE at 40°C of ref. 1. As with LDPE at 40°C the shifts are downwards and to slightly shorter times (see the arrow in *Figure 16F*). So, we think that for this compression moulded PP sample T_g^U lies around 100°C whilst the residual ageing observed in *Figure 16F* is due to crystallization (see refs 1, 3).

From the data in *Figure 16*, we constructed plots of the horizontal and vertical shift rates μ and B (see equations (6) and (7) in ref. 1) and of modulus E and damping $\tan\delta$ at $t=10^3$ s (angular frequency $=10^{-3}\,s^{-1}$) as defined by

$$E=1/F(t) \tag{2}$$

$$\tan\delta=\frac{\pi}{2}\,\mathrm{d}\ln F(t)/\mathrm{d}\ln t \tag{3}$$

(cf. equations (4) and (5) of ref. 1.)

The results, given in *Figure 17* resemble those for another type of PP given in Figure 21 of reference 1. The dashed curves in *Figure 17* have little meaning. They connect the data points at 80 and 120°C in an arbitrary manner (for 100°C, the μ and B values could not be determined).

The present finding of a T_g^U of about 100°C appears to agree with the earlier finding (*Figures 6* and *7*) that the effect of high stresses on ageing disappears at 100–120°C. In our model[1], the effect of the stress level is explained from the erasing of previous ageing of the amorphous phase. But above T_g^U, the amorphous phase

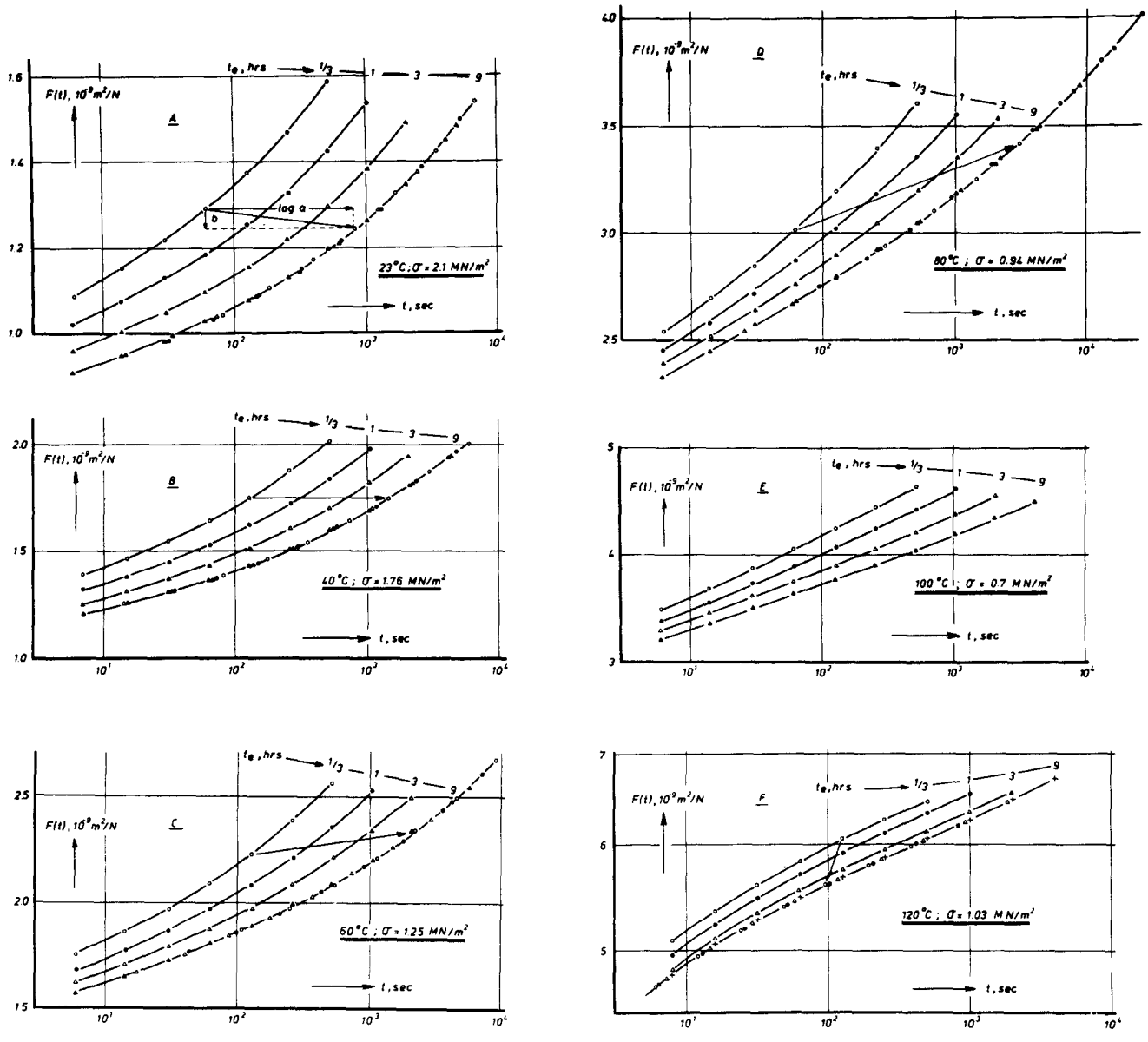

Figure 16 Small strain tensile creep of compression moulded PP, P83M10, quenched from 130°C to various measuring temperatures and tested at t_e values of 0.33–9 h. The master curves were obtained by horizontal and vertical shifts; the arrows denote the shifting direction. At 100°C, the superposition was impossible. (F) (120°C) is double-logarithmic; (A)–(E) are semi-logarithmic

will no longer suffer from ageing effects. Therefore, the effect of the stress level must disappear (as mentioned before, in our model, the residual ageing at 120°C is attributed to crystallization, Figure 8 in ref. 1).

INJECTION MOULDING *versus* COMPRESSION MOULDING

Polypropylene

A comparison of compression and injection moulded PP samples is given in *Figures 18* and *19*. The first shows E and $\tan\delta$ as functions of temperature. Clearly, the injection moulded sample is considerably softer than the compression moulded sample. Moreover, the effects of mould temperature and orientation direction (parallel or perpendicular) are less than the average difference between compression and injection mouldings. This suggests that it is not the frozen-in molecular orientation which is responsible for the differences between the injection and compression moulded samples studied here.

In comparing injection moulded with compression moulded samples, one should particularly realize that the injection mouldings contain an inhomogeneous distribution of molecular orientation and residual stress. The residual stresses may relax with time during storage which causes an additional type of ageing. Such ageing effects should be distinguished from the physical ageing discussed before. The inhomogeneous orientation and stresses are due to the rapidity of the mould filling and cooling process. The usual physical ageing is due to the cooling process proper and also occurs in samples cooled uniformly and not containing residual stresses and orientations.

Whether the inhomogeneities have a large effect on the present data is not known. However, for PVC, we found that for injection mouldings prepared with a high level of internal stress the usual physical ageing is much more important than the effects due to the inhomogeneities (see Figures 26 and 27 of ref. 4). As said before, a similar conclusion is suggested by the data in *Figures 18–19*.

Therefore, we neglect the effect of inhomogeneities here and investigate to what extent the experimental data can be explained from the usual (uniform) ageing process.

The ageing rates μ and B are shown in *Figure 19*. It appears that for the injection mouldings, the transition from region 3 to 4 lies 25°C lower than for the compression mouldings (all curves are displaced by some 25°C to the left). This seems to agree with our model. For the annealed, compression moulded, samples, the crystallinity will be higher than for the injection mouldings. It seems reasonable to assume that the amorphous phase will be the more disturbed the higher the degree of crystallinity. So, in the annealed (compression moulded) samples the glass–rubber transition will be extended to higher temperatures than in the injection mouldings. This reasoning also explains the higher modulus of the compression moulded samples (*Figure 18*). Note further that as in *Figure 18*, in *Figure 19*, the differences due to different injection moulding conditions are smaller than the average differences between compression and injection mouldings.

In view of the above results we conclude that the injection moulded samples have a more mobile (i.e. less restrained) amorphous phase than the annealed, compression moulded, samples. Such an increased mobility is reflected in the long term creep behaviour; an illustration is given in *Figures 20* and *21*. We observe that the injection mouldings are softer, and that their creep rates ($dF/d\log t$) are higher. This agrees with the short-time creep data in *Figure 18*.

The big differences in creep behaviour can be explained quantitatively from the higher mobility of the amorphous phase. In *Figure 22*, we have replotted the short-time parts of the low stress creep curves of *Figures 20* and *21*. The curves for the compression moulded and injection moulded material can be superimposed by shifts that are indicated by the arrows. At 23°C, the mobility is enhanced by a factor of 7, at 40°C by a factor 12.

Just as for amorphous polymers (section 10.3 of ref. 4) such acceleration of the short-time creep leads to a higher slope $dF/d\log t$ in the long term region. The calculation is as follows. For semi-crystalline polymers in regions 2 and 3, momentary creep compliances can be approximated by[3]:

$$F(t)=A+B(t/t_0)^m \tag{4}$$

in which constants A, B, t_0 and m depend on temperature, age and processing conditions.

With an ageing rate μ of 1 (*Figure 19*), the long term creep is found as[3]:

$$\bar{F}(t)=A+B\left(\frac{t_e}{t_0}\right)^m \ln^m(1+t/t_e) \tag{5}$$

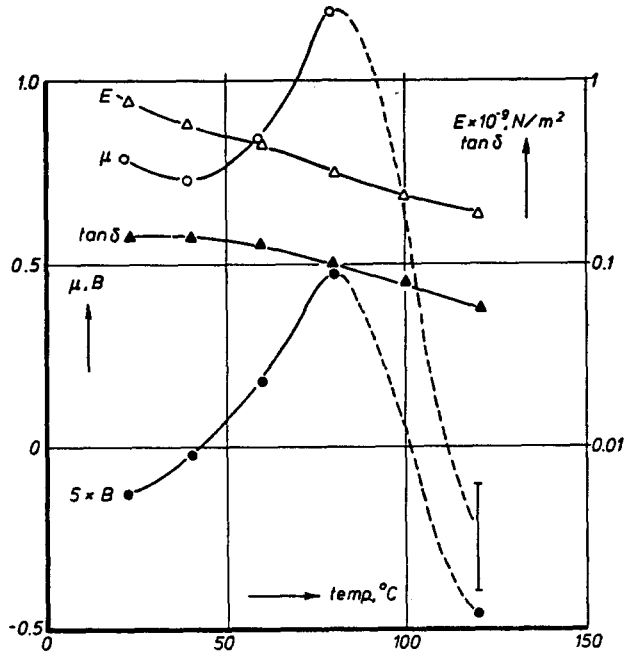

Figure 17 Mechanical and ageing data for compression moulded PP, P83M10, tested at small strains. E and tan δ are given for $t=10^3$ s and $t_e=3$ h. For details, see text

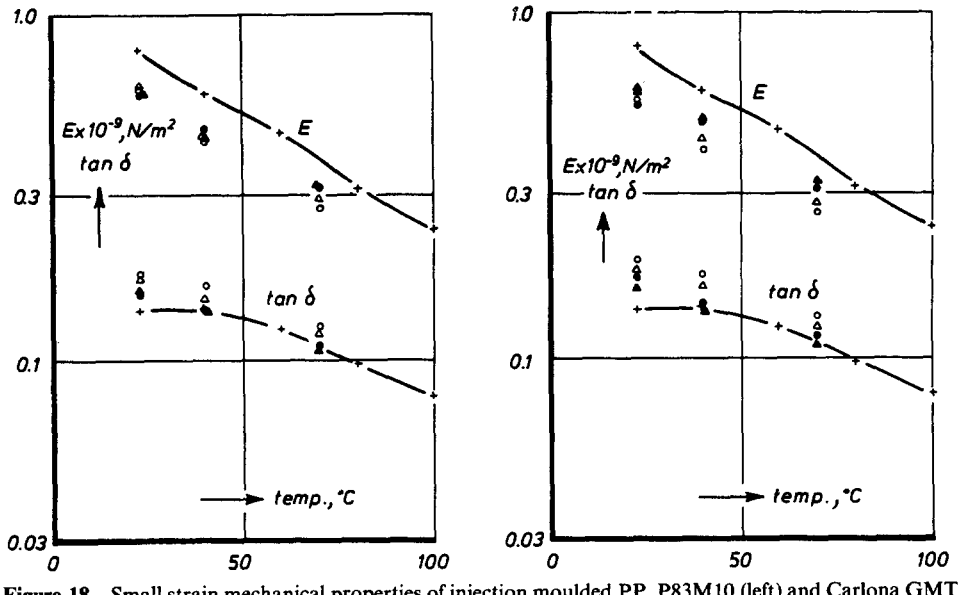

Figure 18 Small strain mechanical properties of injection moulded PP, P83M10 (left) and Carlona GMT 67 (right). E and tan δ are calculated by means of equations (2) and (3); $t=10^3$ s and $t_e=9$ h. Open symbols: samples parallel to flow direction, closed symbols: samples perpendicular to flow direction. ○, $T_m=20$°C; △, $T_m=60$°C. The crosses refer to the compression moulded P83M10. Surprisingly, the modulus is the lowest for samples taken parallel to the (nominal) direction of flow

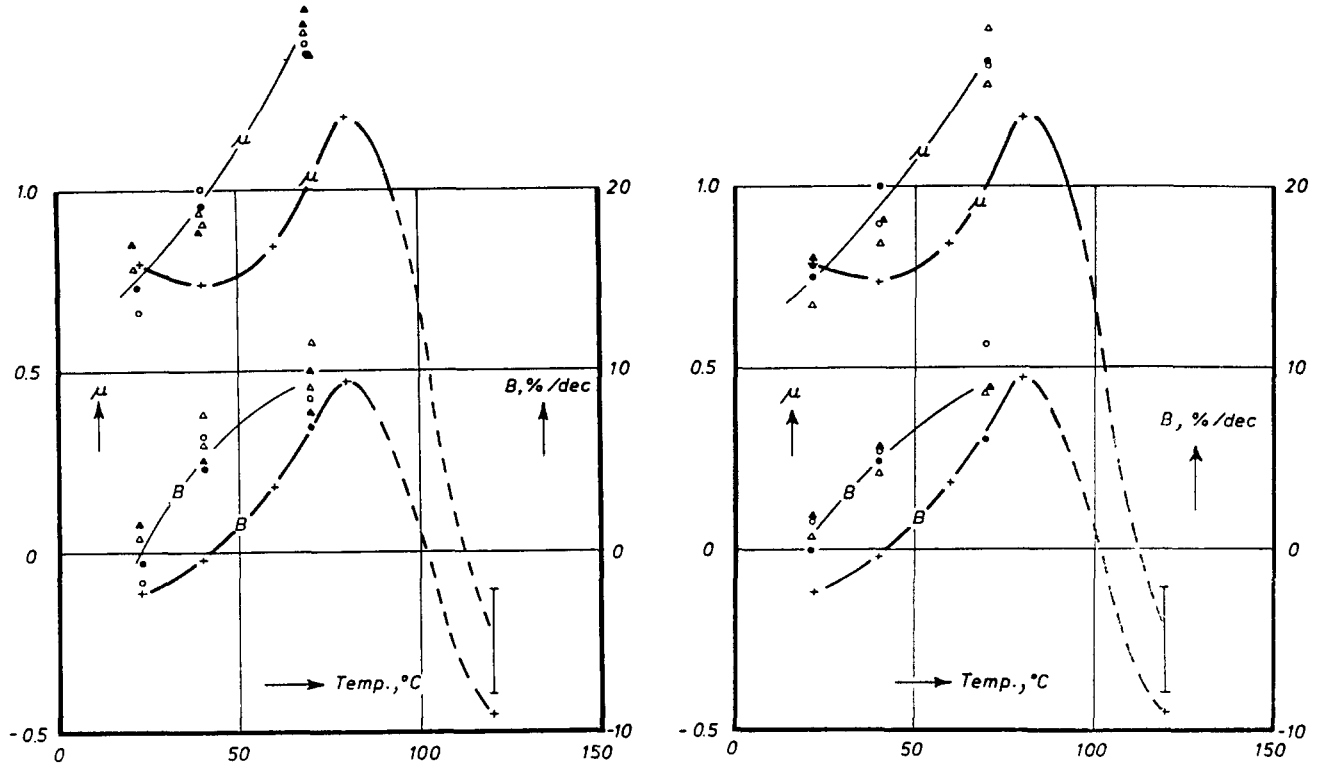

Figure 19 Explanation as for *Figure 18* but for the horizontal and vertical shift rates μ and B. The crosses and heavy curves were taken from *Figure 17*. Left PP, P83M10, right Carlona GMT 67. The meaning of the symbols is as in *Figure 18*

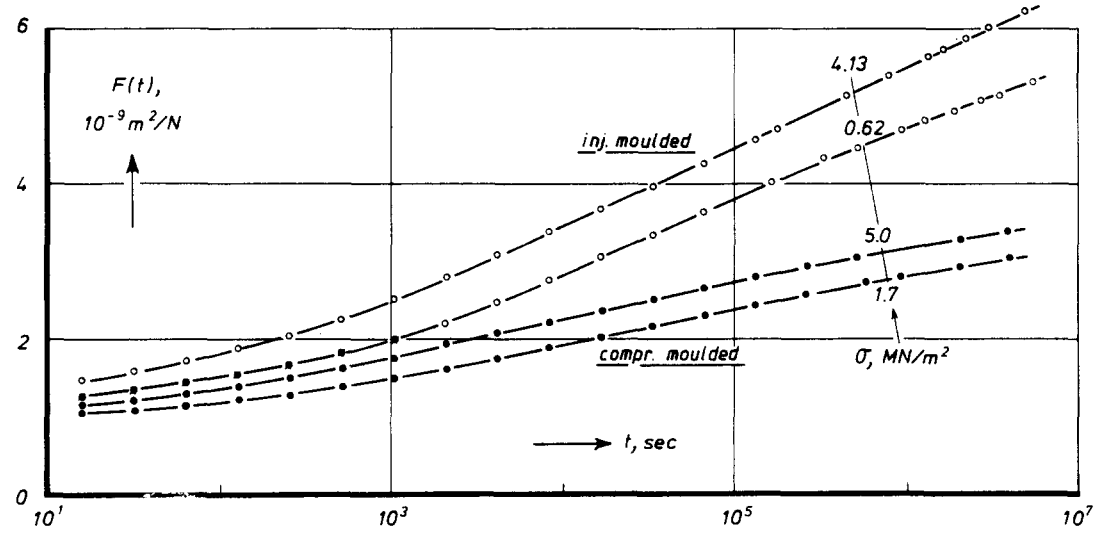

Figure 20 Long term tensile creep of PP, P83M10 at 23°C. The data for the compression moulded samples were taken from *Figure 14* (quench 130↓23°C, $t_e = 1$ h). For the injection mouldings, T_m was 20°C, and the samples were taken parallel to the flow direction. The total storage time at 23°C, including the time used for the milling of the strips, was 1 h

and its rate r as

$$r = \mathrm{d}\bar{F}/\mathrm{d}\ln t = mB\left(\frac{t_e}{t_0}\right)^m \frac{t/t_e}{1+t/t_e} \ln^{m-1}(1+t/t_e) \quad (6)$$

We now compare r_i and r_c (injection and compression moulding, respectively) at equal values of t and t_e. Since $m_i = m_c$ (see *Figure 22* caption) we find from equation (6):

$$\frac{r_i}{r_c} = \frac{B_i}{B_c}\left(\frac{t_{0_c}}{t_{0_i}}\right)^m \quad (7)$$

Because the curves of *Figure 22* are superimposable, we have:

$$A_c + B_c\left(\frac{t}{t_{0_c}}\right)^m = b\left\{A_i + B_i\left(\frac{at}{t_{0_i}}\right)^m\right\} \quad (8)$$

in which a and b are the horizontal and vertical shift factors in *Figure 22* (note that the diagram is double-logarithmic). Equation (8) leads to:

$$\frac{B_i}{B_c}\left(\frac{t_{0_c}}{t_{0_i}}\right)^m = 1/ba^m \quad (9)$$

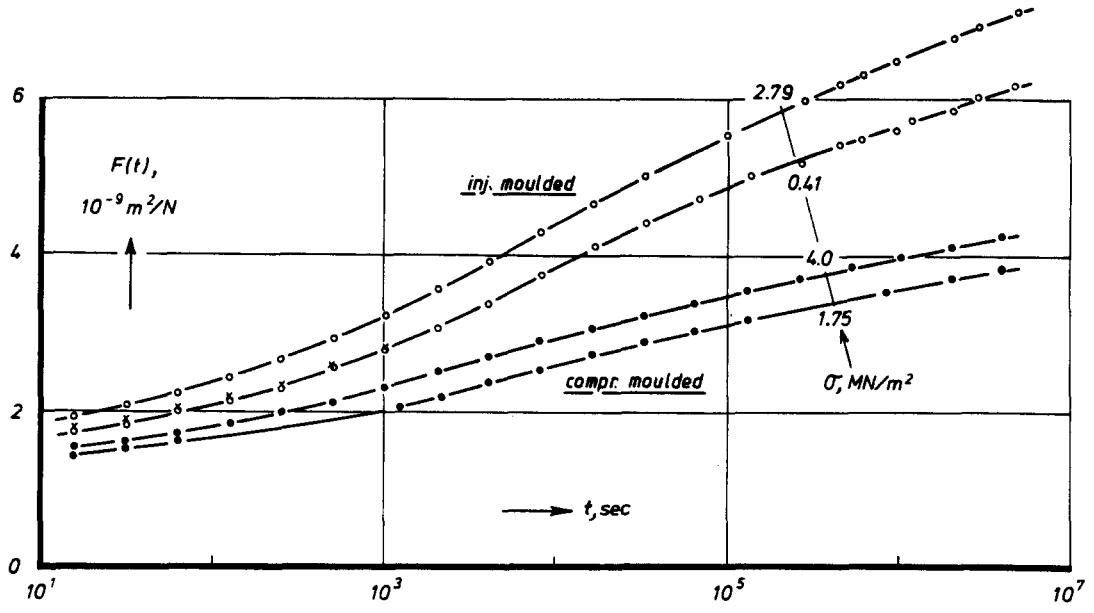

Figure 21 Explanations as for *Figure 20*, but for a measuring temperature of 40°C. The data for the compression moulded samples were taken from *Figure 15*

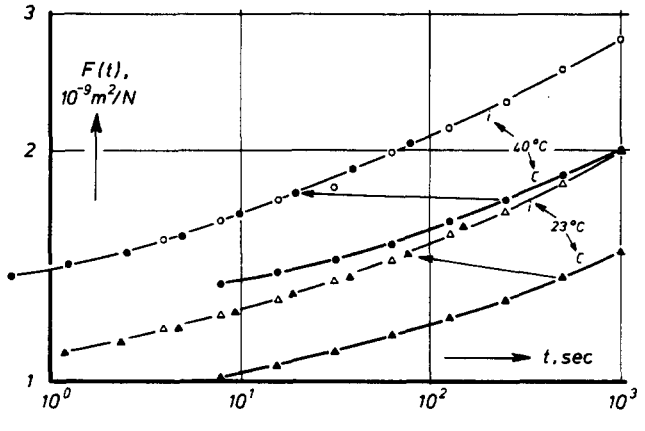

Figure 22 Replot of the short time parts of the creep curves at the lowest stress levels of *Figures 20* and *21*. *c*=compression moulded; *i*=injection moulded. At 23 and 40°C, the *i* and *c* curves could be superimposed. The shifting direction is indicated by the arrows. The superposability implies that the *m* value (equation (4)) is the same for the *i* and *c* curves. A fit of the data to equation (4) yields $m=0.29$ at 23°C and 0.25 at 40°C

Table 2 Ratio of the creep rates r_i and r_c of injection and compression moulded samples, respectively. For details see text. The experimental r_i/r_c data refer to a t value of 10^5 s. The a and b values were taken from *Figure 22*

Temperature, (°C)	m	b	$1/a$	r_i/r_c Equation (9)	r_i/r_c Experimental
23	0.29	0.93	7	1.89	2
40	0.25	0.99	12	1.88	2

Combining equations (7) and (9) we find:

$$\frac{r_i}{r_c}=1/ba^m \qquad (10)$$

A comparison of theory and experiment is given in *Table 2*. Obviously, the agreement is satisfactory, which implies that the differences in long term creep behaviour between injection and compression mouldings can indeed be explained from an enhanced mobility in the amorphous phase.

Polyethylene (HDPE)

A summary of the mechanical and ageing data is given in *Figure 23*. As for PP, the injection moulded sample is softer and the variation in mould temperature has little effect. Further, the transition to region 4 appears to be lowered (as for PP; now to about 50°C). Certainly at 70°C, we have entered into region 4 (both μ and B are negative). It should be realized however that the comparison between the i and c samples is now somewhat ambiguous; the i data refer to Stamylan 9309, the c-data were obtained several years earlier[1] on Stamylan 9400. Yet the picture is consistent with that for PP.

As for PP, the i and c samples strongly differ in their long term creep properties. The data, at 23°C, are presented in *Figure 24*. For $t=10^5$ s, the i sample has crept about three times more than the c sample. Another difference is that for the i sample, the creep curve is no longer straight at long times. A rather sharp decrease in slope occurs at about 8×10^4 s (1 day). In our work, such a bend has only been observed before for LDPE at the transition from region 3 to 4 (cf. Figures 13 and 18 of ref. 1 and Figures 20 and 21 of ref. 3). It might well be that, due to the drop in T_g^U to about 50°C (*Figure 23*), the transition to region 4 becomes visible at 23°C at long times (note that the time scale in *Figure 24* is much longer than in *Figure 23*).

This illustrates the critical remarks made on the linear-extrapolation method in the discussion section of reference 3: during creep there may be a change from region 3 to 4 behaviour. If this is the case for the injection moulded HDPE in *Figure 24*, the prediction of the creep over periods of 10–50 years (i.e. far beyond the bend seen in *Figure 24*), becomes easy: one can simply extrapolate the flat long-time end of the i curve of *Figure 24*. This, in fact, is the method proposed by Moore and Turner previously[7].

A final remark about *Figure 24* is the following. At long times, the creep compliance of the i sample appears

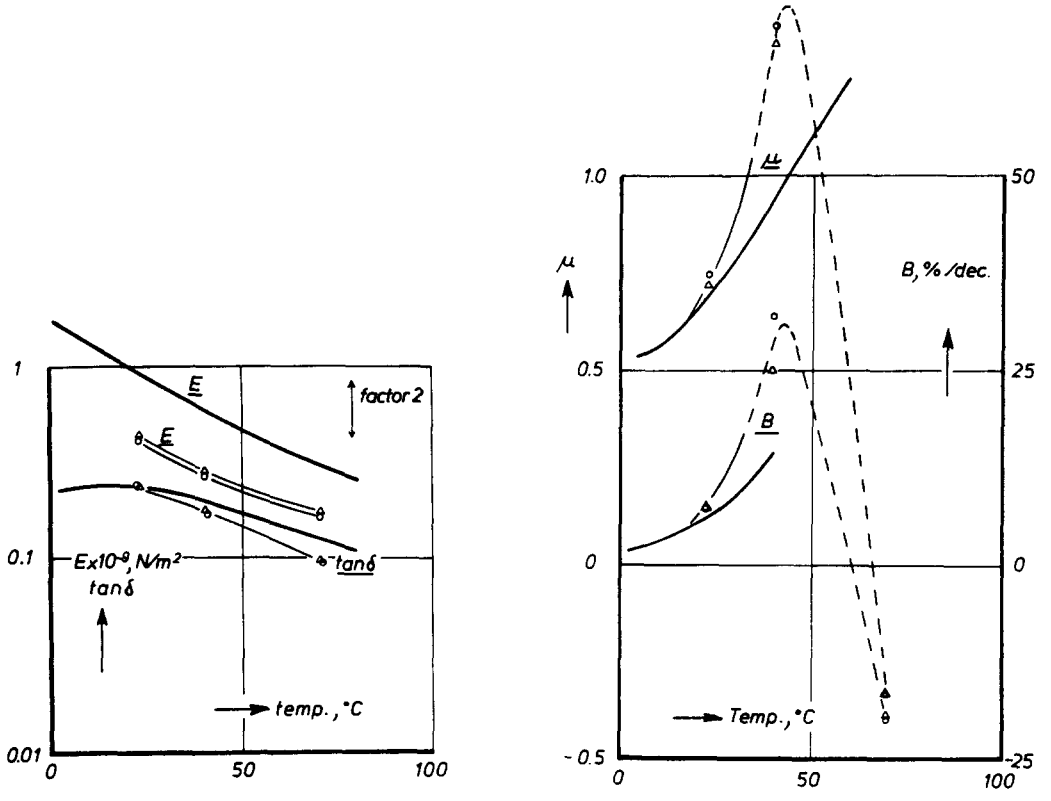

Figure 23 Mechanical (left) and ageing data (right) for HDPE (small-strain data). ———, compression moulded, Stamylan 9400; data from ref. 1; ○, injection moulded, Stamylan 9309, $T_m = 20°C$, parallel to flow; △, injection moulded, Stamylan 9309, but $T_m = 60°C$. E and tan δ refer to $t = 10^3$ s and $t_e = 6$ h

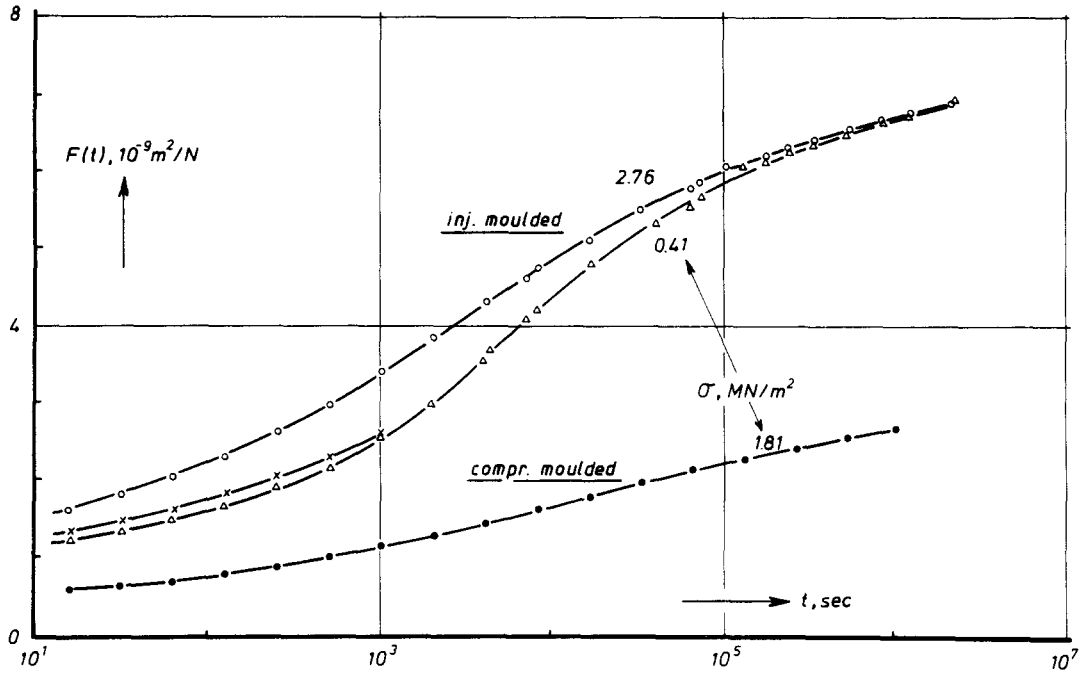

Figure 24 Long term tensile creep of HDPE at 23°C, $t_e = 1$ h. The curve for the compression moulded sample (Stamylan 9400) was taken from Figure 18 of ref. 3. The temperature was 20°C. For the injection moulded sample (taken parallel to flow) T_m was 20°C; material Stamylan 9309

to become independent of stress. This may be another indication for a transition to a region 4 behaviour. The finding is in line with the one discussed earlier, namely the disappearance of the effect of stress level on ageing at temperatures above T_g^U. It also seems to agree with the picture development in reference 4 that the non-linear behaviour of glassy polymers is due to the generation of free volume by shear stresses. Such generation will be absent at temperatures above T_g (here T_g^U).

DISCUSSION

We now arrive at a general discussion of the results reported in the present paper as well as in the three earlier papers[1-3] of this sequence. It seems appropriate to remember the original approach (see pp. 1521–1522 of ref. 1). We simply started from the model of an extended glass–rubber transition, considered the crystalline phase as an inert filler and straightforwardly investigated to

what extent this model could explain the experimental facts. Looking back, it can be concluded that the model is a very useful one. It enables us to rationalize the complex experimental results and to explain the ageing and related phenomena in detail. The essential element in the model is time, i.e. nearly all effects are explained from changes in the mobility in the amorphous phase. Let us recapitulate:

(1) The complicated region 1–4 behaviour naturally follows from the distribution of T_g values. There will be mobile and less mobile regions, and this straightforwardly explains that ageing affects creep by a combination of horizontal and vertical shifts (Figures 5–7 of ref. 1). It also naturally follows that, with increasing temperature, we first have horizontal shifts (region 1), then a downward shifting (region 2), then an upward shifting (region 3) and finally a disappearance of the horizontal shifts (region 4). It also directly follows that time–temperature superposition applies to regions 1 and 4 but not to region 3.
(2) Since the amorphous phase is partially glassy, we naturally expect the following similarities with purely amorphous polymers: the retrograde shifting and the reversals in shifting direction which occur upon heating (partially) aged samples (Figure 13 of ref. 2) and the erasing of previous ageing by high stresses.
(3) The decrease in mobility with age directly explains that long term creep curves become more or less straight (strain versus log t) for $t > t_e$ (see ref. 3 and the long term data in the present paper).
(4) Rapid cooling from the melt will result in a less restrained amorphous phase. Therefore the distribution of T_g values narrows and at some given high temperature T, a rapidly cooled sample will show less ageing than a slowly cooled material. For the rapidly cooled material T may be above T_g^U (no ageing), whereas for the slowly cooled material T may lie below T_g^U. So, there is a temperature range in which the ageing effects will be intensified by pre-annealing and slow cooling notwithstanding the fact that pre-annealing already has caused a stiffening and a decrease in creep rate.
(5) The ageing of filled rubber systems[2] directly follows from the model.

In fact, experimental findings disagreeing with the model were not encountered so far. One may object that the model is so versatile that it can explain everything. We think that such an objection is incorrect; too many details are correctly predicted and apparent deviations could be fitted consistently after all. Some examples include the disappearance of the effect of stress on ageing at 120°C (*Figures 6–7*) which could be explained from the fact that for PP, T_g^U lies at 100°C and the bend in the long term creep of injection moulded HDPE (*Figure 24*) which could be explained from the very low T_g^U in this material. So, we conclude that the model gives a satisfactory description of the ageing behaviour of semi-crystalline polymers.

It should be realized that the present model deviates considerably from the usual thinking. Often, semi-crystalline polymers are considered as two-phase composites; one phase is crystalline and the other amorphous. The amorphous phase is supposed to show a glass transition similar to that of a bulk amorphous polymer. Such glass transitions are sharp (about 10°C) and

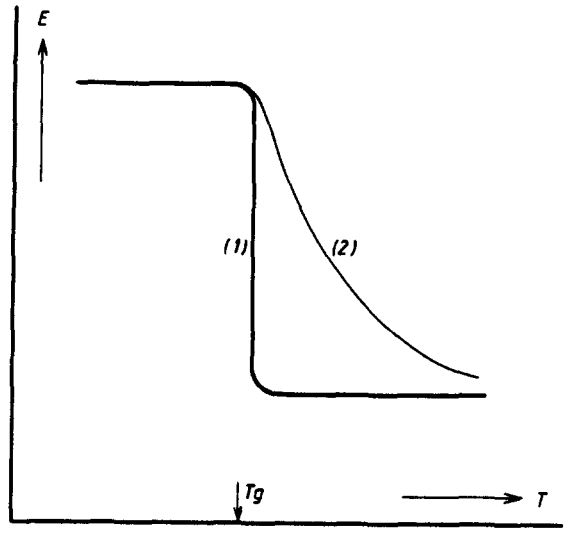

Figure 25 Modulus *versus* temperature for semi-crystalline polymers; for details see text. Curve 1, usual model; curve 2, present model

therefore, the usual picture leads to a modulus–temperature plot as shown by curve 1 in *Figure 25*. The present model (distribution of T_g values) leads to curve 2.

Polymers such as PE and PP do not reveal curve 1 but curve 2[8,9], and this is naturally explained by the present model. In the usual model, curve 2 is explained from relaxation phenomena in the crystalline phase, or at the interface between amorphous and crystalline material[8–12]. To some extent one is forced to such an explanation because the rubbery amorphous phase is considered to be free of relaxations. So, if our model is correct, the usual interpretations of, for example, the α-transition in PE and PP should be reconsidered.

In the usual model, the ageing effects (above T_g) can be explained from secondary crystallization. The degree of crystallinity X_c is supposed to increase and therefore the material stiffens. It is very difficult to see how this could explain our experimental data. The natural consequence of a stiffening is a downward shifting of the creep curves. So, this model does not explain the fact that ageing mainly effects changes in mobility (i.e. horizontal shifts). Of course, one can argue that changes in X_c also cause changes in mobility. However in doing so, one has to explain why the second-order effect (changes in mobility) overshadows the first-order effect (stiffening). Moreover, we cannot see how the complex region 1–4 behaviour (upward shifts in region 3, downward shifts in regions 2 and 4) can be explained in this way.

There are three other points which are difficult to understand from the model of secondary crystallization. These are discussed below.

The continuity at the conventional T_g *of the semi-crystalline polymer.* The data in reference 1 show that ageing and volume relaxation are continuous at the conventional T_g of the semi-crystalline material. There are no indications for a change in mechanism. Our model naturally explains this continuity. In the secondary crystallization model the continuity at T_g forces one to explain the ageing below T_g from crystallization as well. This, however, is highly improbable. Firstly, experiments have shown that for some semi-crystalline polymers the ageing below T_g is not accompanied by changes in X_c (ref. 13). Secondly, the ageing below T_g of a semi-crystalline polymer is very similar to that in purely

amorphous polymers such as PS and PMMA. Finally, as long as we assume that a part of the semi-crystalline polymer is amorphous, this amorphous phase must show ageing effects below T_g (all amorphous materials show ageing below T_g (ref. 4)). So, crystallization cannot be the sole cause of ageing below T_g. Consequently, we lose the continuity at T_g if crystallization is considered as the sole cause of ageing above T_g. We then have crystallization above T_g and amorphous-phase ageing plus crystallization below T_g. In our model, the change in (ageing) mechanism occurs at T_g^U, and this change is clearly revealed by the experimental data (μ drops to zero or negative values, B drops from positive to (large) negative values, the creep curves change shape and above T_g^U time–temperature superposition becomes feasible again).

The density dependence of the modulus during ageing at $T > T_g$. From the ageing and volume relaxation tests, we can calculate the percentage change in compliance J per percent change in specific volume v; in the formula:

$$\mathrm{d}\ln J/\mathrm{d}\ln v = \frac{\left(-\frac{1}{J}\frac{\mathrm{d}J}{\mathrm{d}\log t_e}\right)}{-\frac{1}{v}\frac{\mathrm{d}v}{\mathrm{d}\log t_e}} = \frac{\rho}{\beta} \qquad (10)$$

Some results are given in *Table 3*. For HDPE, LDPE and PP, the ρ-values were taken from Figures 11–13 of reference 1 (creep time $t = 256$ s), the β-values as well as the indications about the region type (fourth column) from Figures 19–21 of reference 1. The POM data were from unpublished results. The seventh column of *Table 3* shows that for isothermal ageing, the $\mathrm{d}\ln J/\mathrm{d}\ln v$ values range from 160 to 2250, so a 0.1% change in density is accompanied by a change in stiffness of 16 to 225%.

This sensitivity can be compared with that found when the density is varied by heat treatments aimed to change the degree of crystallinity. Such values were taken from the literature and are given in the last column of *Table 3*. Clearly, a density change due to a change in crystallinity, produced by high temperature annealing, has a much smaller effect on stiffness (order of 5–10) than the density changes which occur during isothermal ageing at low or moderate temperatures (this can also be seen in Figures 8.6 and 8.10 of reference 15; a similar conclusion can be found in the literature[16]). So, if crystallization were the cause of the ageing effects above T_g, this sensitivity problem has to be solved.

The lowest values (160 and 180) for ρ/β found in *Table 3* are those for LDPE at 40°C and PP at 80°C. For LDPE, a value as low as 100 has even been found at 60°C (not shown in *Table 3*). These values are much closer to the values of 25–50 given in the last column of *Table 3* than are the ρ/β values found at lower temperatures. This seems to agree with the earlier findings about the T_g^U values in LDPE and PP. For LDPE the ageing at $T > 30$°C is assumed to be due to secondary crystallization[1] and for PP, the temperature of 80°C is also close to T_g^U.

The temperature range of ageing. Our model predicts that the ageing effects will occur over a wider temperature region when T_g^U is increased, for example, by an increase in X_c by high temperature annealing. If ageing were caused by crystallization, one would expect the opposite. Most of the experimental evidence has already been discussed. Here, we would like to mention some additional points.

The data in Figure 25 in reference 1 show that at 100–120°C the ageing is stronger in the nucleated than in the unnucleated Nylon 6. Table 1 in reference 1 shows that for the first material X_c is considerably higher than for the second. Also the differences between LDPE and HDPE can be interpreted in this way. For HDPE, X_c is much higher than for LDPE (Table 1 of reference 1) and the ageing effects are indeed found over a much wider temperature range (Figures 19 and 20 in reference 1).

Altogether we conclude that the crystallization model is not the best candidate for explaining the ageing of crystalline polymers above their conventional T_g. To this should be added that several authors[16–18] came to the same conclusion on the basis of a measurement of X_c during for example, the room temperature ageing of PP. No changes in X_c could be detected. The opposite, however, has also been claimed[19].

It should be remembered that the basic idea of two or more T_g values (distribution) in semi-crystalline polymers is not new. It has been described extensively by Boyer in 1973[20–21]. Boyer's discussion concentrates on two separate T_g values, but he points out that a distribution

Table 3 Dependence of compliance J on specific volume v as calculated from ageing and volume relaxation (ρ/β) and as estimated from literature data about the effect of crystallization on J (last column)

Polymer	Nr[a]	Temperature	Region	ρ	$\beta \times 10^4$	$\mathrm{d}\ln J/\mathrm{d}\ln v = \rho/\beta$	$(\mathrm{d}\ln J/\mathrm{d}\ln v)_{cr}$
HDPE	40	−100	1	0.045	0.2	2250	
		− 40	1	0.087	3.1	280	25–40[b]
		+ 40	3	0.13	2.2	590	−50[c]
LDPE	41	− 60	1/2	0.110	2.2	510	
		0	2/3	0.164	4.0	410	
		+ 40	4	0.121	7.4	160	
PP	43	− 20	1	0.13	2.0	650	35–45[d]
		+ 20	2	0.154	6.2	250	
		+ 80	3	0.089	5.0	180	
POM	42	20	2	0.099	3.8	258	22–40[e]

[a] Code number in reference 1
[b] From ~1 Hz torsional pendulum plots between −50 and +50°C for polyethylenes with a crystallinity varying from 69–85%[14]
[c] From the differences between HDPE and LDPE in the isochronous stress–strain curves at 100 s and 20°C (Figure 8.10 in reference 15)
[d] From isochronous stress–strain curves at 20°C and 100 s (Figure 7.4 and p. 63 of reference 15) and from ~1 Hz torsional pendulum plots between 0 and 100°C for PP with densities varying from 0.880–0.905 g cm^{-3} (p. 378 of reference 8)
[e] From ~1 Hz torsional pendulum plots between −70 and 100°C for POM with densities varying from 1.404–1.444 g cm^{-3} (p. 541 of reference 8)

of T_g values is equally possible and, in fact, more natural[21]. Further, Menczel and Wunderlich[22] recently showed (on the basis of d.s.c. measurements) that, above the conventional T_g, the amorphous phase of a semi-crystalline polymer consists of a 'rigid' (glassy) and a 'mobile' (rubbery) part. The fraction of rigid material may be larger than that of the mobile amorphous material. The rigid material 'devitrifies' at a temperature (our T_g^U) considerably higher than T_g. For poly(butylene terephthalate) the authors could show that T_g^U increases with the degree of crystallinity (see also Boyer[21]).

Let us complete this paper by mentioning some unresolved problems. For PE and PP, the T_g^U is connected with a peak in the mechanical loss factor tan δ (cf. Figures 19–21 of reference 1). This peak must be identified with the well known α peak, extensively described in the literature[8–12]. It is known that this peak consists of two parts: a high temperature α_2 peak which originates from motions in the crystals (this peak is also found in single crystal mats) and a low temperature component α_1 which is explained from motions within the crystals (deformations of intermosaic block regions[10]) or from molecular motions at the crystal/amorphous interface[9]. The α_2 peak has an activation energy H of 45 kcal mol^{-1}. For the α_1 peak, H values of 25–31 kcal mol^{-1} are reported[10]. Both peaks shift with frequency according to an Arrhenius equation.

It is also known that the intensity of the α_1 component strongly increases when, due to a lowering of the measuring frequency, the α_1 peak shifts to lower temperatures[10]. This effect on the peak intensity is immediately explained when the α_1 peak is identified as 'our' T_g^U peak. With increasing temperature the amount of 'rigid' amorphous material decreases, and the tan δ peak caused by the 'devitrification' of this rigid material decreases in height (compare Figure 9 in reference 1 and note that tan δ is proportional to the slope of the creep curve). What actually causes a problem is the low value of the activation energy. In our model, α_1 is a kind of glass–rubber transition. For amorphous polymers, such transitions possess much higher (apparent) activation energies. Moreover the behaviour is strongly non-Arrhenius (H increases with decreasing temperature). This point should be clarified in the future. Possibly, the literature data on the activation energies of the α_1 and α_2 peak are not very reliable. The data are found after splitting a composite peak into two components which implies that a lot of assumptions are needed to find the activation energies.

The low apparent activation energy of the α_1 peak process may cause problems in the practical application of the methods for predicting long term creep[3]. Suppose, that at short times (say 1000 s) the transition to a region 4 behaviour lies at 100°C. The difference in $1/T$ between 100 and 23°C is only 0.70×10^{-3}. So, with an activation energy of 25 kcal mol^{-1}, we expect a time shift $\log a = (\Delta(1/T))H/(2.303R)$ of only four decades. Consequently, the transition to a region 4 behaviour would be found at 10^7 s (about 4 months) at room temperature. This would invalidate long term creep predictions based on linear extrapolation (region 3 behaviour; compare the discussion section of reference 3 and the results in the section on polyethylene in the present paper). If the transition to region 4 occurs at moderate times (weeks to months), we can better use the prediction method designed for region 4 which is, in fact, very similar to the one proposed previously by Moore and Turner[7] (see reference 3).

CONCLUSIONS

For semi-crystalline polymers, the effect of previous ageing diminishes when the stress level in the creep tests is increased. The behaviour is the same as in amorphous polymers. The methods for predicting the long term creep of semi-crystalline polymers can be generalized to the non-linear high stress regime.

Rapid cooling, as in injection moulding, produces softer samples than compression moulding followed by annealing. The creep resistance may decrease by a factor of 2–3. These effects can be explained from an enhanced mobility in the amorphous phase.

The model of an extended glass transition in semi-crystalline polymers appears to be supported by all experimental data presented in parts 1–4 of the present sequence of papers[1–3].

ACKNOWLEDGEMENTS

The author wishes to acknowledge DSM for sponsoring the work reported here in the year 1976. He is also indebted to Mrs C. Zoeteweij, Mrs M. P. Bree and Mr R. W. van Hoesen Korndorffer for carefully performing the experiments.

REFERENCES

1 Struik, L. C. E. *Polymer* 1987, **28**, 1521
2 Struik, L. C. E. *Polymer* 1987, **28**, 1533
3 Struik, L. C. E. *Polymer* 1989, **30**, 799
4 Struik, L. C. E. 'Physical Aging of Amorphous Polymers and Other Materials', Elsevier, Amsterdam, 1978
5 Struik, L. C. E. in 'Failure of Plastics', (Eds W. Brostow and R. D. Corneliussen), Hanser, Munich, (1986)
6 Struik, L. C. E. *Polymer* 1980, **21**, 962
7 Moore, D. R. and Turner, S. *Plastics and Polymers* 1974, 41
8 McCrum, N. G., Read, B. E. and Williams, G. 'Anelastic and Dielectric Effects in Polymeric Solids', Wiley, London, (1967)
9 McCrum, N. G. in 'Molecular Basis of Transitions and Relaxations', (Ed. D. J. Meier), Gordon and Breach, London, (1978)
10 Kajiyama, T., Okada, T., Sakoda, A. and Takayanagi, M. *J. Macromol. Sci. (Phys.)* 1973, **B7**, 583
11 Stein, R. S. *Macromol. Sci. (Phys.)* 1973, **B8**, 29
12 Tanaka, A., Chang, E. P., Delf, B., Kimura, I. and Stein, R. S. *J. Polym. Sci. (Phys.)* 1973, **11**, 1891
13 Ito, E., Yamamoto, K., Kobayashi, Y. and Hatakeyama, T. *Polymer* 1978, **19**, 39
14 Stehling, F. C. and Mandelkern, L. *Macromolecules* 1970, **3**, 242
15 Ogorkiewicz, R. M. 'Engineering Properties of Thermoplastics', Wiley-Interscience, London (1970)
16 Schael, G. W. *J. Appl. Polymer Sci.* 1966, **10**, 901
17 Gezovich, D. M. and Geil, P. M. *Polym. Eng. Science* 1968, **8**, 202
18 Agarwal, M. K. and Schultz, J. M. *Polym. Eng. Sci.* 1981, **21**, 776
19 Busfield, W. and Blake, C. S. *Polymer* 1980, **21**, 35
20 Boyer, R. F. *Macromolecules* 1973, **6**, 288
21 Boyer, R. F. *J. Macromol. Sci. (Phys.)* 1973, **B8**, 503
22 Menczel, J. and Wunderlich, B. *ACS Polym. Prepr.* 1986, **27**, 255